Fottea, Olomouc, 23(2): 149–163, 2023
DOI: 10.5507/fot.2022.021

Unravelling the hidden complexity in diversity and pigment composition of a colonial flagellate *Synura sphagnicola* (Chrysophyceae, Stramenopiles)

Pavel Škaloud[1*], Magda Škaloudová[1], Iva Jadrná[1], Jana Pilátová[2,3], Woonnghi Shin[4] & Jiří Kopecký[5]

[1] *Charles University, Faculty of Science, Department of Botany, 12800 Praha 2, Czech Republic; [*]Corresponding author e–mail: skaloud@natur.cuni.cz*
[2] *Charles University, Faculty of Science, Department of Experimental Plant Biology, 12800 Praha 2, Czech Republic*
[3] *Charles University, Faculty of Mathematics and Physics, Institute of Physics, Division of Biomolecular Physics, 12000 Praha 2, Czech Republic*
[4] *Chungnam National University, Department of Biology, 34141 Daejeon, Korea*
[5] *Laboratory of Algal Biotechnology – Centre ALGATECH, Institute of Microbiology of the Czech Academy of Sciences, Opatovický mlýn, 379 81 Třeboň, Czech Republic*

Abstract: In this study, we aim to taxonomically evaluate a unique example of cryptic diversity in a freshwater protist species *Synura sphagnicola*, occurring at two evolutionary levels. First, we characterize two species, *S. sphagnicola* and *S. rubra* sp. nov., that diverged from one another approx. 14 Mya. These species are morphologically well differentiated by the morphology of silica scales. Second, we propose seven evolutionary young, but ecologically and geographically well differentiated lineages as separate sub–species, *sphagnicola*, *agilis*, *borealis* (within *S. sphagnicola*), *rubra*, *ampla*, *bella* and *caelica* (within *S. rubra*). In addition, we examine the autofluorescence and pigment composition of two selected strains, identifying fucoxanthin as a predominant carotenoid. We further show that the red droplets in the cytoplasm, a prominent feature of both species, are formed by a previously unknown pigment. Finally, we identify chlorophyll–c_2 in *S. sphagnicola*. Since the lack of this pigment represents a major distinguishing character to discriminate between classes Synurophyceae and Chrysophyceae, we formally synonymize these taxa.

Key words: cryptic diversity, evolution, molecular phylogeny, morphology, pigments, Synura, Synurophyceae, taxonomy

Introduction

Synura sphagnicola (Korshikov) Korshikov (Chrysophyceae, Synurales) is a colonial, cosmopolitan, silica–scaled flagellate originally described from peat bogs near Zvenigorod, Moscow district, Russia as *Skadovskiella sphagnicola* Korshikov, including figures of its scales (Korshikov 1927). Two years later, Korshikov clarified his observations and transferred *Skadovskiella sphagnicola* to the genus *Synura* Ehrenberg (Korshikov 1929). Later on, the detailed information on scale and cell ultrastructure of *Synura sphagnicola* based on electron microscopic (EM) examination was published by Petersen & Hansen (1958) and Hibberd (1978). The expanding availability of EM to phycologists initiated a plethora of floristic and ecological studies which often found *S. sphagnicola* dominant in slightly to very acidic waters (Siver 1989; Kristiansen & Preisig 2007). More recently, with the continuing development of molecular methods, *S. sphagnicola* was inferred to represent a distinct, genetically quite separate lineage within the section Curtispinae of *Synura* (Jo et al. 2016). Pusztai et al. (2016) showed *Synura synuroidea* (Prowse) Pusztai, Čertnerová, Škaloudová et Škaloud, formerly described as *Chrysodidymus* Prowse, to be a sister clade of *Synura sphagnicola*.

Recently, a detailed investigation of *S. sphagnicola* diversity was published by Škaloud et al. (2019), based on the collection of 71 strains isolated from various water bodies from Europe, Newfoundland and Korea. According to the multilocus phylogenetic analysis, *S. sphagnicola* was shown to split into two distinct lineages referred to as sp1 and sp2, approximately 15.4 million years ago. In addition, Škaloud et al. (2019) reported a rapid diversification of both lineages into several geographically

and ecologically diverse incipient species that occurred during the late Pleistocene.

Both *S. sphagnicola* lineages and *S. synuroidea* are remarkable by a permanent presence of red droplets in the cytoplasm (Korshikov 1927; Conrad 1939; Harris & Bradley 1958; Graham et al. 1993; Pusztai et al. 2016). These droplets, occasionally observed also in related species *S. curtispina* (Petersen et Hansen) Asmund (Andersen 2010), and *S. spinosa* Korshikov (our observations), are situated mainly at the anterior end of the cell. Though red droplets represent a prominent feature present in these above–mentioned taxa, their nature is still not known. In the old literature these droplets are referred to as an accumulation of haematochrome (Korshikov 1927; Conrad 1939), which is however an obsolete term for a mixture of carotenoid pigments and their derivates.

The major aim of this study was to taxonomically evaluate the uncovered diversity within the *S. sphagnicola* morphotype. We recognized the lineages sp1 and sp2 as two separate species, and further described several evolutionary young, incipient species as sub–species taxa. In addition, we used fluorescence microscopy and high–performance liquid chromatography (HPLC) analyses to examine the pigment composition of both *S. sphagnicola* lineages in order to characterize the nature of their enigmatic red droplets.

Material and Methods

Investigated strains. The origin and sampling details of *Synura* strains used in this study are described in Škaloud et al. (2019). In addition, we further investigated four newly obtained strains: NIES 695, Hudong11291J2, K35 and M44 strains (for origin see Supplementary Table 1). All strains were cultured in 50 ml Erlenmeyer flasks filled with the MES buffered DY IV liquid medium (pH ≈ 6; Andersen et al. 2005), at 15 °C, under constant illumination of 40 $\mu mol.m^{-2}.s^{-1}$ (TLD 18W/33 fluorescent lamps, Philips, Amsterdam, the Netherlands).

Sequencing and phylogenetic analysis. A total of seven molecular loci were sequenced for newly obtained strains: nuclear (nu) ITS rDNA, 18S rDNA, 26S rDNA, plastid (pt) 23S rDNA, rbcL, psaA, and mitochondrial (mt) coxI. DNA isolation and amplification was performed as described in Škaloud et al. (2020). Multiple alignments of above–mentioned loci sequences were constructed using MAFFT v6, applying the Q–INS–i strategy (Katoh et al. 2002). The positions with deletions prevailing in a majority of sequences were removed from the alignment. Two phylogenetic analyses were performed as follows.

First, a concatenated nu–18S rDNA, nu–26S rDNA, pt–23S rDNA, pt–rbcL and pt–psaA was prepared to infer the phylogeny of the genus *Synura*, using *Neotessella* as an outgroup (Supplementary Table 1). Prior to performing the concatenated phylogenetic analysis, maximum likelihood (ML) analyses were performed separately for each locus to verify there are no obvious topological incongruencies among the loci. The ML analyses were performed using RAxML 8.1.20, using the default GTR+Γ evolutionary model. Bootstrap analyses were performed with the rapid bootstrapping procedure, using 100 pseudoreplicates. The analyses were shown to be highly congruent in statistically supported lineages (bootstraps >70). Accordingly, the concatenated analysis was performed on the partitioned alignment, separating all loci as well as three codon positions in protein–coding pt–rbcL and pt–psaA genes. Statistical significance of inferred phylogeny was further evaluated by maximum parsimony (MP) analysis and Bayesian inference (BI). The MP bootstrapping was performed using PAUP v.4.0b10 (Swofford 2003) by heuristic searches with 1000 random sequence addition replicates and random addition of sequences. The bootstrap support values were obtained from 100 pseudoreplicates, respectively. BI was performed using MrBayes v.3.2.6 (Ronquist et al. 2012), carried out on partitioned datasets applying the substitution models described in Škaloud et al. (2020). Two parallel MCMC runs were carried out for eight million generations, each with one cold and three heated chains. Convergence of the two cold chains was assessed during the run by calculating the average standard deviation of split frequencies (SDSF). The SDSF value between simultaneous runs was 0.0016.

Second, the species tree analysis was performed on *S. sphagnicola* nu–ITS rDNA, pt–psaA, and mt–coxI sequences, using the StarBEAST template in BEAST2 v.2.4.7 (Bouckaert et al. 2014). Eight haplotypes were defined in taxon set, including haplotypes sp1A, sp1B, sp1C, sp1D, sp2A, sp2B, sp2C described in Škaloud et al. (2019), and a newly recovered haplotype sp1E representing the strain NIES 695. MCMC analyses were run for 100 million generations, using the setting as described in Škaloud et al. (2019). To infer node divergence times, the clock rates for ITS rDNA (9.569×10^{-3}), psaA (2.571×10^{-3}) and coxI (4.962×10^{-2}) loci were specified based on fossil data estimations published by Škaloud et al. (2019).

The trees were analysed in DensiTree (Bouckaert 2010) and the trees showing the most likely tree topology were drawn, along with the consensus tree.

Morphological analyses of silica scales. The morphological analyses were based on seventeen cultures selected in both the lineage sp1 (nine cultures) and sp2 (ten cultures), respectively. The cultures were inoculated into fresh media, and after 4–5 weeks of cultivation they were examined with a JEOL 1011 transmission electron microscope. For each of these cultures, the five characters were measured in at least 30 randomly selected scales, as follows: (1) scale length, (2) scale width, (3) spine length, (4) spine width near its base, and (5) rim width at the lower–most portion of the scale. The same characters were measured in figures illustrating the iconotypes of scales of *S. sphagnicola* and *S. bioretii* Huber–Pestalozzi in the papers of Korshikov (1927) and Huber–Pestalozzi (1941). Statistical analyses were performed in R 4.2.0 (R Core Team 2021). First, a Principal Component Analysis (PCA) was performed on 926 morphologically characterized scales, analysing all five measured morphological traits. Second, the PCA was performed on the same dataset of 926 scales supplemented by ten iconotypes of *S. sphagnicola* and *S. bioretii*. Since it was impossible to measure the exact dimensions of iconotype scales due to the absence of scale bars and rather illustrative nature of drawings, we analysed the three relative values only, as follows: (1) scale length to width ratio, (2) scale length to spine length ratio, (3) scale width to spine length ratio. The PCA ordinations were plotted using the vegan (Oksanen et al. 2020) and labdsv (Roberts 2019) packages in R. In addition, we performed a Linear Discriminant Analysis (LDA) using the MASS package

(Venables & Ripley 2002). All five measured morphological traits were analysed. The LDA scores were visualized using the ggplot2 (Wickham 2016) and ggridges (Wilke 2021) packages. The confusion matrix was then calculated to measure the performance of the model. This matrix reports the number of cases correctly and incorrectly assigned to each of the groups based on the discriminant analysis.

Ecological analyses. To test for ecological differentiation of particular sp1 and sp2 haplotypes, we obtained climatic data for 51 *S. sphagnicola* strains with known geographic origins and genotype affiliations (Supplementary Table 2). Altitude and 19 bioclimatic variables were obtained from the WorldClim database (Hijmans et al. 2005) at resolution of 2.5 arc minutes to characterize the general climatic conditions. Seven physical and chemical soil properties (pH in water, cation exchange capacity, clay, silt and sand content, and organic carbon stock and content were obtained from the SoilGrids database (soilgrids.org) to characterize bedrock properties. Prior to the analysis, forward selection by redundancy analysis was used to reduce the number of predictors, using the ordiR2step function in vegan package in R. Finally, we performed the LDA analysis as described above, based on standardized variables.

Morphological and fluorescence analyses of cells. Cells of strains Hudong11291J2 (sp1) and M44 (sp2) were observed regularly under the Olympus BX51 light microscope equipped by Canon EOS 700D camera. The strains grown for three weeks were also observed for their fluorescent properties, using Olympus Provis AX70 microscope equipped by mercury lamp, an appropriate fluorescent block (U–MWU), and Nikon D3100 DSLR camera. Fluorescent micrographs contrasting was adjusted in Photoshop CS5. For better resolved emission spectra, we used an alpha300 RSA laser scanning confocal microscope (WITec, Germany) equipped with a 442 nm laser set to 10 μW power, Olympus UPlanFL N Oil 100× NA = 1.3 and spectrometer UHTS300S VIS with grating 600 g.mm^{-1} set for spectral in situ stitching of emission spectra in the range of 445 to 800 nm averaging five measurements of 0.7 ms integration time. Data were analysed using WITec Project FIVE Plus v5.1 software.

Pigment extraction. Organic solvents for pigment extraction and HPLC analyses were obtained from Analytika (Czech Republic). All solutions were prepared using reverse–osmosis deionized water (Ultrapur, Watrex, Prague, Czech Republic). For the pigment analyses the *Synura* cells were removed from culture medium by centrifugation for 10 min at 4.500×g. The sediment was homogenized with glass beads in vortex and extracted twice at room temperature with 100% acetone for 15 min. The combined extracts were clarified using 0.2 μm nylon filters (Micro–spin centrifuge filter, Alltech, Deerfield, IL, USA). All other chemicals used were of analytical grade and were purchased from Sigma–Aldrich.

HPLC/DAD/MS. The extracts were analysed on a Dionex UltiMate 3000 UHPLC (Thermo Scientific, Sunnyvale, CA, USA) equipped with a diode array detector (DAD) and Impact HD high resolution mass spectrometer (Bruker, Billerica, Massachusetts, USA) with electrospray ionization source (ESI). The following settings of MS were used: drying temperature 250 °C; drying gas flow 12 l.min^{-1}; nebulizer gas pressure 4 bar; capillary voltage 4000 V; endplate offset 500 V. The spectra were collected in the range 20–2200 m.z^{-1} with spectra rate of 3 Hz. Collision energy was 35 eV. Mass spectrometer was calibrated with sodium formate clusters and LockMass. Tuning Mix (622 Da) was used as the lockmass calibrant at the beginning of each analysis. The formulas of obtained molecular peaks and fragments were calculated using Smart Formula in Bruker Compass DataAnalysis software (version 4.2).

Pigments were separated using a modified method of Van Heukelem & Thomas (2001) on the Luna C8(2) 100 Å column (100 × 4.6 mm, 3 μm, Phenomenex) thermostated to 30 °C, with binary solvent system (0 min 100% A, 20 min 100% B, 25 min 100% B, 27 min 100% A, 30 min 100% A, where A is 80% methanol and B is 100% methanol). The solvent flow rate was 0.8 ml.min^{-1}. Injection volume was 20 μl. The identification of the carotenoids was performed, considering the combination of the following parameters: elution order on the reverse phase column, UV–vis spectrum features (maximum absorption wavelength (λ_{max}), spectral fine structure (%III/II) and peak cis intensity (%Ab/AII)), MS and MS/MS spectra characteristics and data available in the literature.

Results

Phylogenetic analyses

Congruently with the analysis published by Škaloud et al. (2019), *S. sphagnicola* strains were inferred to form two distinct, well–resolved sister clades, referred to as sp1 and sp2 (Fig. 1A). The split of these clades was estimated to 14.0 [5.6–29.8] Mya, which is similar to the estimate of 15.4 [8–25] Mya given by Škaloud et al. (2019). The clades were separated by a long branch from the remaining *Synura* species of the section Curtispinae (*S. synuroidea*, *S. spinosa*, *S. curtispina*, and *S. longitubularis* Jo, Shin, Kim et Siver). The coalescence species tree analysis recovered the existence of eight haplotypes, five within the clade s1 and the remaining three within the clade s2 (Fig. 1B). The coalescence analysis was consistent with that published by Škaloud et al. (2019) with the exception of recovering a novel haplotype sp1E representing the strain NIES 695 (Supplementary Table 1). The haplotypes were inferred to be evolutionary very young, with their age spanning from 20,000 to 80,000 years.

Morphological analyses of silica scales

The principal component analysis (PCA) of silica scales characteristics based on measurement of 17 strains clearly separated the sp1 and sp2 lineages (Fig. 2A). The lineages were morphologically well differentiated by most of the measured characters, namely scale length and width, rim width and spine length, which were correlated with the PC1 axis (Figs 2B–D). The linear discriminant analysis (LDA) also showed a clear separation of sp1 and sp2 lineages along the first LD axis (Fig. 2E). The accuracy of the model was 0.92, meaning that 92% of the scales were correctly assigned to the appropriate clade based on the morphological traits only.

To determine which of the two inferred lineages indeed represent *S. sphagnicola*, we further performed the PCA supplemented by *S. sphagnicola* scales

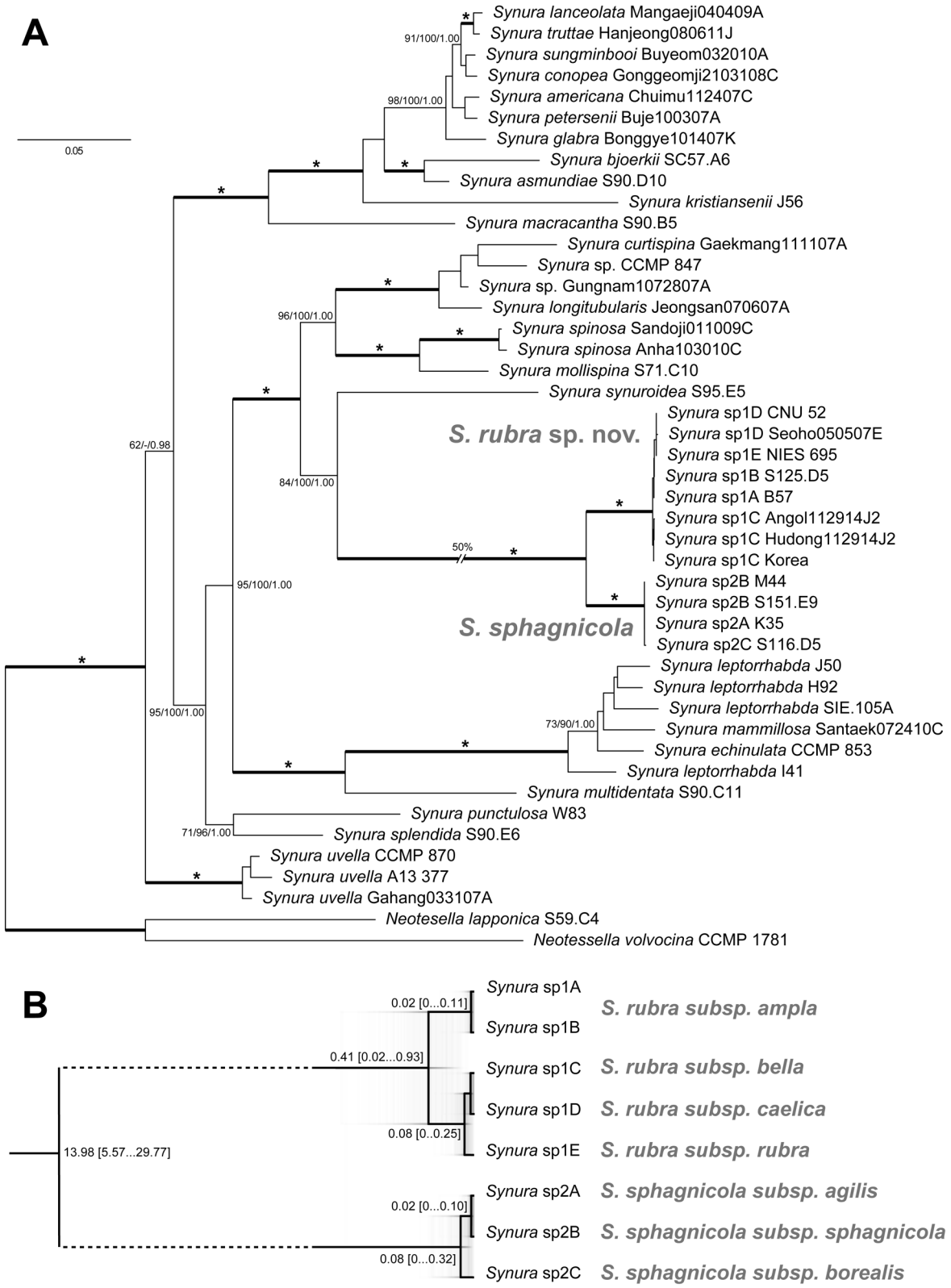

Fig. 1. Phylogenetic position and relationships of *S. sphagnicola* strains. (A) Phylogeny of the genus *Synura* based on concatenated nuclear 18S rDNA, 26S rDNA, and plastid 23S rDNA, rbcL, and psaA sequences; values at the nodes indicate statistical support estimated by three methods; MrBayes posterior node probability (left), maximum likelihood bootstrap (middle) and weighted maximum parsimony bootstrap (right); thick branches with asterisks highlight nodes receiving the highest statistical supports (1.00/100/100); scale bar represents the expected number of substitutions per site; (B) time–calibrated coalescence species tree with visualization of the consensus topology, based on ITS rDNA, psaA and coxI sequences; mean divergence times are given for selected nodes, along with 95% highest posterior density (HPD) values in square brackets.

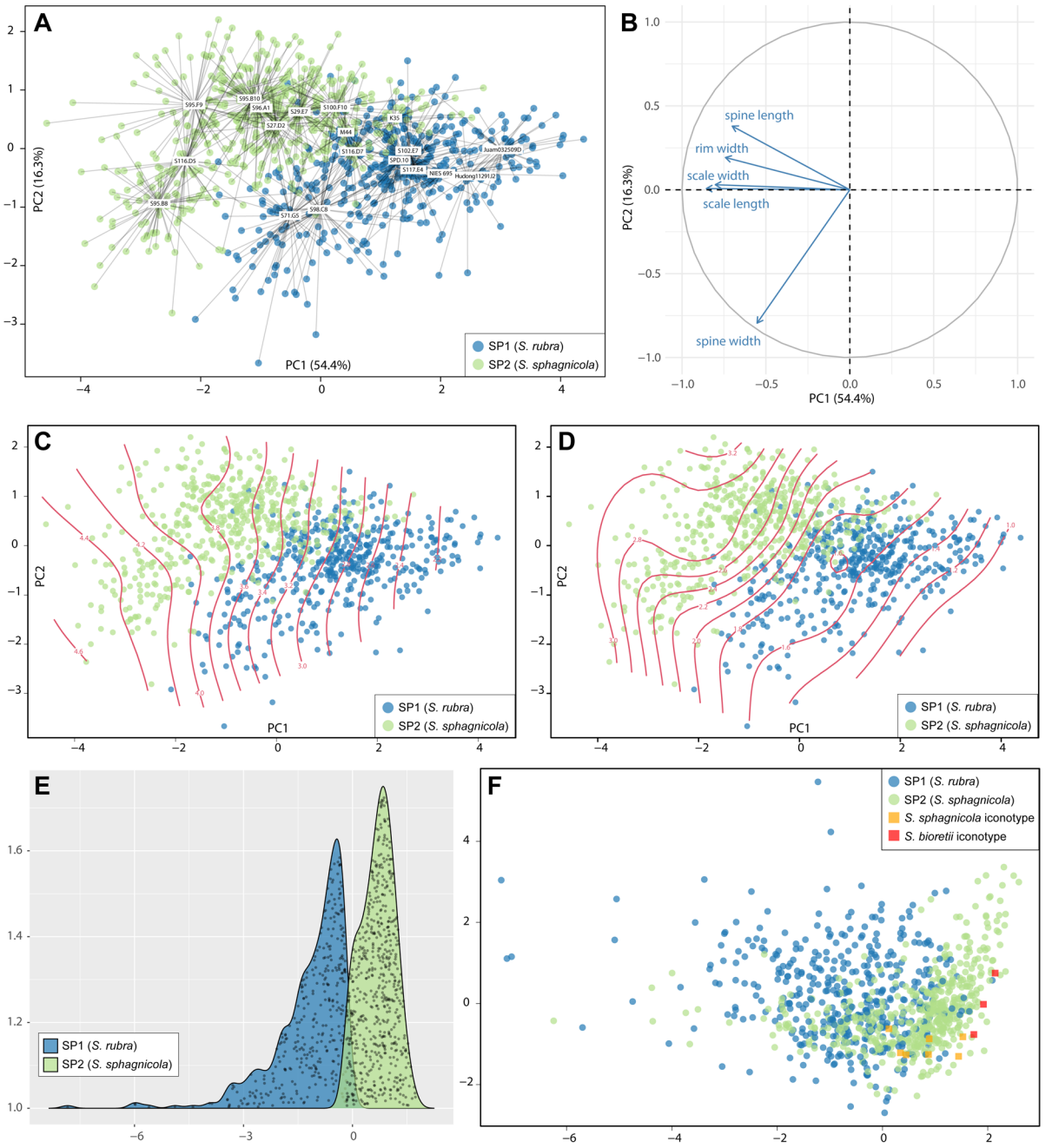

Fig. 2. Morphological analyses of silica scales. (A) principal component analysis (PCA) based on five morphological traits measured on 926 scales, showing differentiation of sp1 (*S. rubra*, sp. nov.) and sp2 (*S. sphagnicola*) lineages; the scales are clustered based on their affiliation to 17 investigated strains; (B) correlation of morphological variables with PCA axes; (C, D) contour plots showing the relationships between PCA scores and scale (C) and spine lengths (D); (E) linear discriminant analysis (LDA) showing morphological differentiation of lineages; (F) PCA analysis based on three morphological traits measured on 926 scales and ten iconotypes of *S. sphagnicola* and *S. bioretii*.

illustrated by Korshikov (1927) and representing the species iconotype. In addition, we included the originally illustrated scales of morphologically similar species *S. bioretii* (Huber–Pestalozzi 1941). The scales of both species were inferred to morphologically correspond to the lineage sp2 (Fig. 2F). Indeed, a classification matrix computed by LDA assigned all ten iconotype scales to the lineage sp2. The posterior probabilities for the lineage sp2 ranged 0.63–0.86 and 0.87–0.88 for *S. sphagnicola* and *S. bioretii*, respectively.

Ecological differentiation of haplotypes.
Most of the haplotypes within the sp1 and sp2 lineages were morphologically indistinguishable. However, with the exception of haplotypes sp1A and sp1B they clearly differ by climatic and bedrock preferences. Within the lineage sp1, mean diurnal range, maximum temperature of warmest month, annual precipitation, precipitation of wettest month and warmest quarter, altitude, and pH were identified as major drivers of haplotype differentiation (Fig. 3A). The accuracy of the LDA model was 0.83,

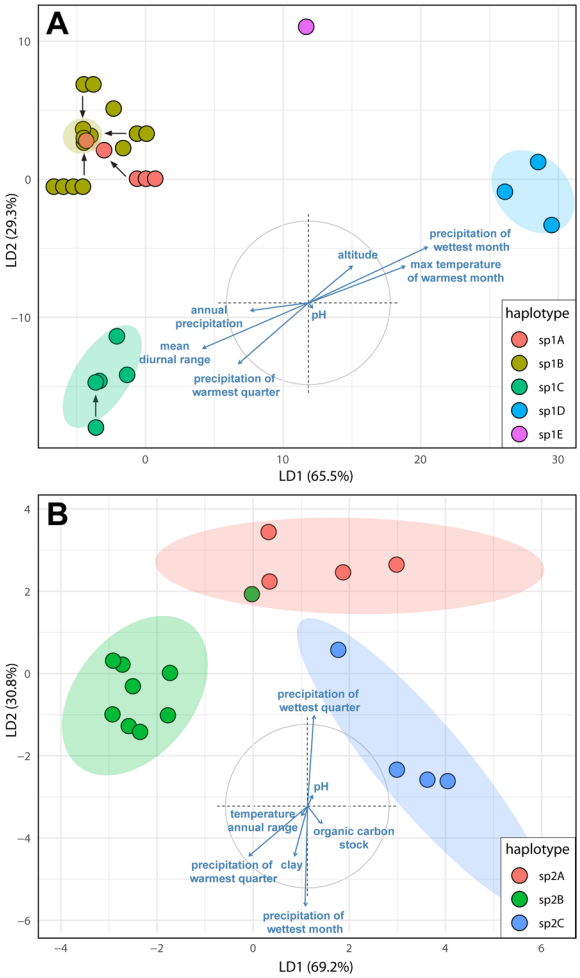

Fig. 3. Ecological differentiation of haplotypes. (A) LDA analysis of sp1 (*S. rubra*, sp. nov.) haplotypes based on seven ecological parameters selected by forward selection; (B) LDA analysis of sp2 (*S. sphagnicola*) haplotypes based on seven ecological parameters selected by forward selection; correlations of environmental variables with the first and second PCA axes are shown within the plots.

meaning that 83% of the strains were correctly assigned to the appropriate haplotype based on the climatic data. However, when treating the sp1A and sp1B as a single haplotype (sp1AB), the accuracy of the model increases to 1.00. Accordingly, all four haplotypes are well differentiated based on their ecology. Whereas the haplotype sp1AB occurs in dry environments, haplotype sp1E prefers much humid climate (Fig. 4A). The haplotypes sp1AB and sp1E also prefer more acidic localities (Fig. 4B). The haplotype 1C can be well differentiated by occurring in those environments showing high diurnal range (high differences between day and night temperatures; Fig. 4C). Similarly, the sp2 haplotypes clearly differentiated by their ecology. Temperature annual range, precipitation of wettest quarter, warmest month and wettest month, as well as pH, clay content and organic carbon stock were identified as major drivers of haplotype differentiation (Fig. 3B). The haplotype sp2B prefers those environments showing high temperature annual range (high differences between the hottest and the coldest months; Fig. 4D), as well as habitats with lower organic carbon stock (Fig. 4E). The sp2C haplotype occurs in areas with lower temperature and higher precipitation in wettest months (Fig. 4F). The accuracy of the LDA model was 0.91.

Light microscopy

The colonies and cells of both sp1 and sp2 lineages shared a very similar morphology. Colonies of sp1 lineage were 29–34 µm in diameter, mostly composed of 8–16 cells (Fig. 5A). Cells were rounded, distinctly spiny, with rather small, pale green chloroplasts filling less than a half of the cell content. The storage products (probably chrysolaminaran (=chrysolaminarin, leucosin), HIBBERD 1978) were deposited in droplets in the posterior part of the cell. In the old cells, storage products could fill a high portion of the cell volume (Fig. 5B). Colonies of sp2 lineage were 32–40 µm in diameter, mostly composed of 8–16 cells (Fig. 5C). Cells were rounded, distinctly spiny, with pale green to brownish chloroplasts filling at least half of the cell content. Similar to sp1 lineage, the storage products were first deposited in droplets, filling a high portion of the cell volume (Fig. 5D). Cells of both lineages had two flagella of almost equal length, one of them having a distinct undulating appearance (Figs 5E, G). The most prominent feature of both lineages was the presence of distinct red or red–violet droplets, first occurring at the apical part of the cell (Fig. 5F), later on produced beneath the entire cell membrane (Fig. 5H).

Fluorescence of *Synura* cells

Under fluorescence microscope using UV excitation, we detected (i) blue autofluorescence of some enigmatic droplets and/or diffusively present in the cytoplasm, (ii) green autofluorescence of the flagellum, (iii) red autofluorescence of plastids and (iv) rather inconspicuous dark red autofluorescence of red droplets, that changed over the course of observation towards orange–yellow (Figs 5I–L). To address the spectral properties of autofluorescence in *Synura*, their emission spectra were measured by a laser scanning confocal microscope with 442 nm laser excitation in situ that limited the observation of the blue autofluorescence (Figs 5M, N). The spectra of sp1 and sp2 lineages were highly congruent. First, green autofluorescence of the narrow, not undulating flagellum was observed in both lineages and in both cases with the prominent flagellar swelling supposedly acting in photoreception and phototaxis. The relatively less intense green fluorescence of flagella peaked between 490 and 500 nm. Second, in both lineages, the strongest fluorescence emission was detected between 660 and 720 nm corresponding to chlorophyll. Third, the dark red fluorescence appearing in red droplets was caused by its low intensity rather than an emission wavelength clearly distinguishable from the plastids, showing wide emission spectra ranging from 580 to 710 nm (expressed as the full width at half–maximum) with a peak in 640 nm.

Table 1. Identification of major pigments present in *Synura* strains.

R_t [min.]	Pigment	Absorption maxima [nm]	$[M+H]^+$	Fragments
5.0	**unknown pigment**	292, **494-500**	967	653, 339
			983	669, 355
			999	685, 371
6.7	Chlorophyll–c_2	**449**, 582, 635	**609,2718**	591.2624, 549.1838
9.4	Fucoxantin	**450**	**659,4349**	641.4265, 623.4127, 581.4021, 563.3923
10.6	Neoxanthin	416, **440**, 468	**601,4189**	583.4588, 565.4195, 509.3618
11.7	cis-Fucoxantin	**334**, **442**	**659,4352**	641.4246, 623.4130, 581.4018, 563.3967
12.7	Unknown carotenoid	422, 446, 472	601,4277	–
14.5	Zeaxantin	**452**, 476	**569,4344**	551.5106, 489.3749, 477.3748, 416.4050
20.4	Chlorophyll–a	**432**, **666**	**893,5469**	614.2410, 583.2214, 555.2273, 481.1904
22.2	Phaeophytin–a	**410**, 508, 538, 608, **666**	**871,5767**	593.2787, 533.2575
23.3	β-Carotene	**450**, 474	**537,4481**	457.3897, 413.3222

Pigment composition

The lineages sp1 and sp2 showed highly congruent elution profiles of the pigments, though their relative abundances significantly differed (Fig. 6). Identification of the individual pigments is given in the Table 1. Fucoxanthin with retention time (Rt) = 9.4 min represented the dominant pigment of the lineage sp1. Interestingly, in the lineage sp2 fucoxanthin was overrepresented by so far unknown pigment with Rt = 5.0 min. This pigment was detected in the lineage sp1, as well, however, in a much lower abundance. Other pigments detected include chlorophyll–c_2 (Rt = 6.7 min), neoxanthin (Rt = 10.6 min.), cis–fucoxanthin (Rt = 11.7 min), zeaxanthin (Rt = 14.5 min), chlorophyll–a (Rt = 20.4 min), and β–carotene (Rt = 23.3 min).

Discussion

Taxonomic consequences

Synura sphagnicola represents a unique example of cryptic diversity in protists, occurring at two evolutionary levels. First, two evolutionary older lineages, here referred to as sp1 and sp2, evolved approximately 14 million years ago. Here, we pointed out that these lineages can be morphologically differentiated by detailed analyses of silica scales, in particular by scale dimensions and spine length (Figs 2B, D). Second, several very young genotypes were detected in both lineages, diverging 20,000 to 80,000 years ago. Since all but one genotypes clearly differ ecologically (Figs 3, 4) and in their distribution pattern (Škaloud et al. 2019), we hypothesise they represent very young, incipient species–level lineages. Contrary to evolutionary older cryptic species of microalgae, reports on much recent species divergences are extremely scarce (Logares et al. 2007; Annenkova et al. 2015), apparently due to the absence of any distinguishing morphological traits. Nevertheless, in the case of ecologically differentiated *S. sphagnicola* genotypes, the above data lead us to believe that these are young but already fully differentiated species that arose during the last glaciation period due to adaptation to various climatic oscillations (Hewitt 2000) or due to differences in their geographical distribution. To distinguish between these two evolutionary levels of speciation, we propose here to describe evolutionary older lineages as two separate species, while more recently evolved, ecologically distinct genotypes as their subspecies. With the exception of ecologically identical genotypes sp1A and sp1B considered here as a single subspecies, the ecological distinction of all other genotypes warrants their recognition as separate subspecies.

Prior to formal description of selected evolutionary older lineage as a new species, it is necessary to i) identify which of two lineages represents *S. sphagnicola*, and ii) check if the second lineage corresponds to any previously described species. A total of five *Synura* species are known to produce red droplets in the cytoplasm: *S. curtispina*, *S. spinosa*, *S. synuroidea*, *S. sphagnicola*, and *S. bioretii*. Only the last species remains to be characterized genetically. Based on the morphometric analyses of species' iconotypes (Fig. 2F), both *S. sphagnicola* and *S. bioretii* morphologically correspond to the lineage sp2. Since *S. bioretii* was described after the description of *S. sphagnicola*, the former represents a junior synonym of the latter. The

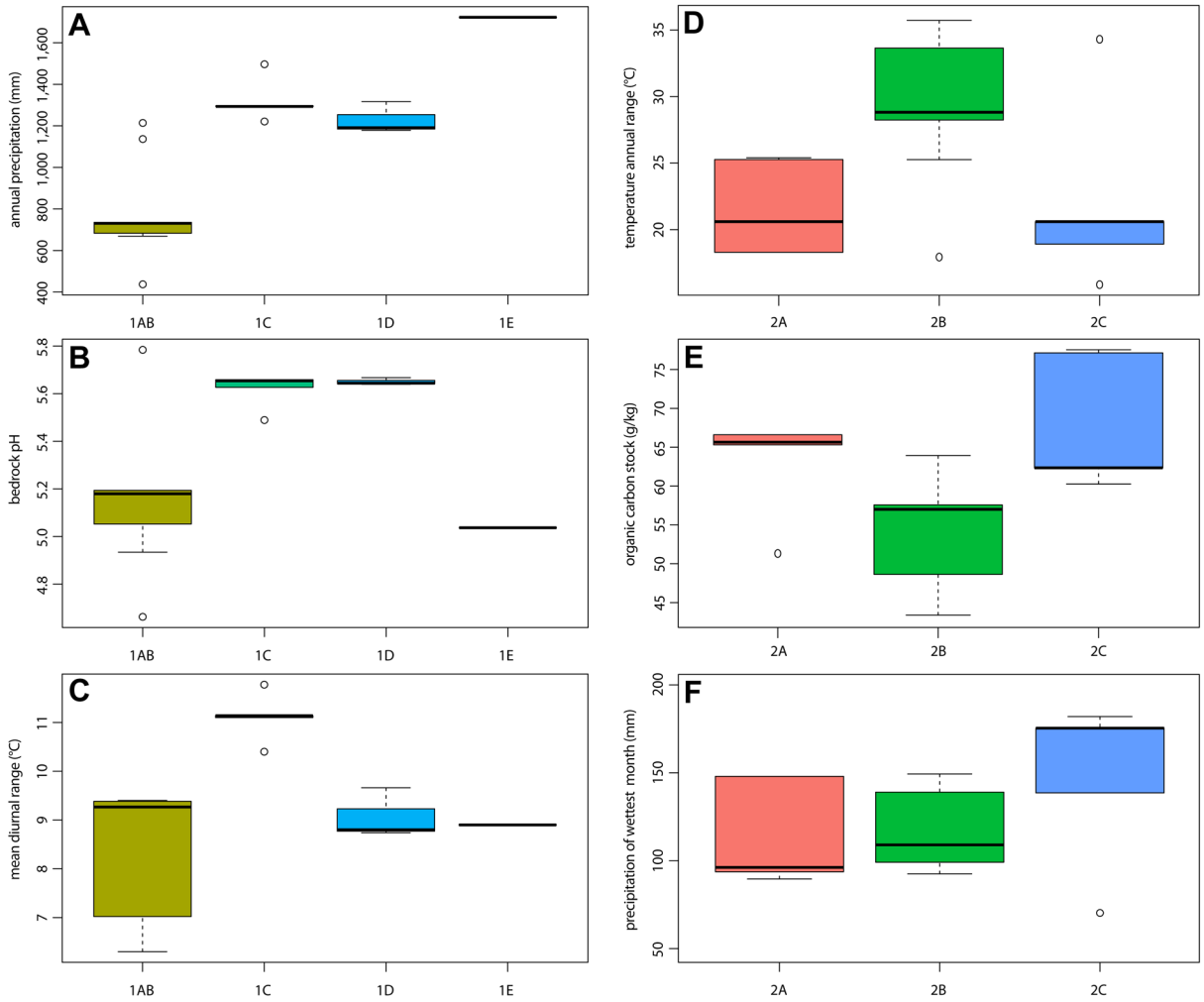

Fig. 4. Ecological preferences of *Synura* haplotypes. (A–C) Differences in the distribution of four sp1 (*S. rubra* sp. nov.) haplotypes along the gradients of (A) annual precipitation (BIO12), (B) bedrock pH, and (C) mean diurnal range (BIO2); (D–F) differences in the distribution of four sp2 (*S. sphagnicola*) haplotypes along the gradients of (D) temperature annual range (BIO7), (E) organic carbon stock, and (F) precipitation of wettest month (BIO13).

sp1 lineage then represents a new, undescribed species, proposed here as *Synura rubra* sp. nov. (see Taxonomic revisions and diagnoses below).

Autofluorescence in *Synura* cells

The enigmatic blue autofluorescence may correspond to multiple cellular compartments and/or substrates, and its exact composition is therefore difficult to address. Based on the literature, blue autofluorescence is a distinct feature of compounds possessing conjugated systems of double bounds or aromatic rings in their structures under UV excitation, i.e., pyridine nucleotides (e.g., nicotine–amide–adenine–dinucleotide (phosphate)), pterins, phenolics (e.g., flavones, coumarins etc.), alkaloids, tyrosine oxidation products, amyloid and non–amyloid protein aggregates etc. (HUANG et al. 2002; ROSCHINA 2012; FRICANO et al. 2019; DONALDSON 2020).

Green autofluorescence of the short (posterior) flagellum is a common feature in brown and golden algae and has been previously well documented in *Synura petersenii* and *S. synuroidea* (= *Chrysodidymus synuroideus*; KAWAI 1988; GRAHAM et al. 1993). Maximum intensity of autofluorescence is concentrated on the base of the flagellum. Here is a swelling that is considered to be a photoreceptive site for phototaxis (KREIMER 1994). The fluorescent flagellar substance was attributed to flavin(s) in the flavoprotein (FUJITA et al. 2005). We observed autofluorescence throughout the flagellum (Figs 5J, L), however, our repetitive examination of several *S. sphagnicola* strains revealed its fluctuating character. In some cells, and especially in these from old cultures, the green autofluorescence was weak or even absent. We recognized that its absence relates to the formation of palmelloid stages where cells lose their flagella.

Fluorescence pattern of plastids containing the complex mixture of photosynthetic pigments of chlorophyll–a and c together with carotenoids correspond to emission spectra reported elsewhere (SILKINA et al. 2009).

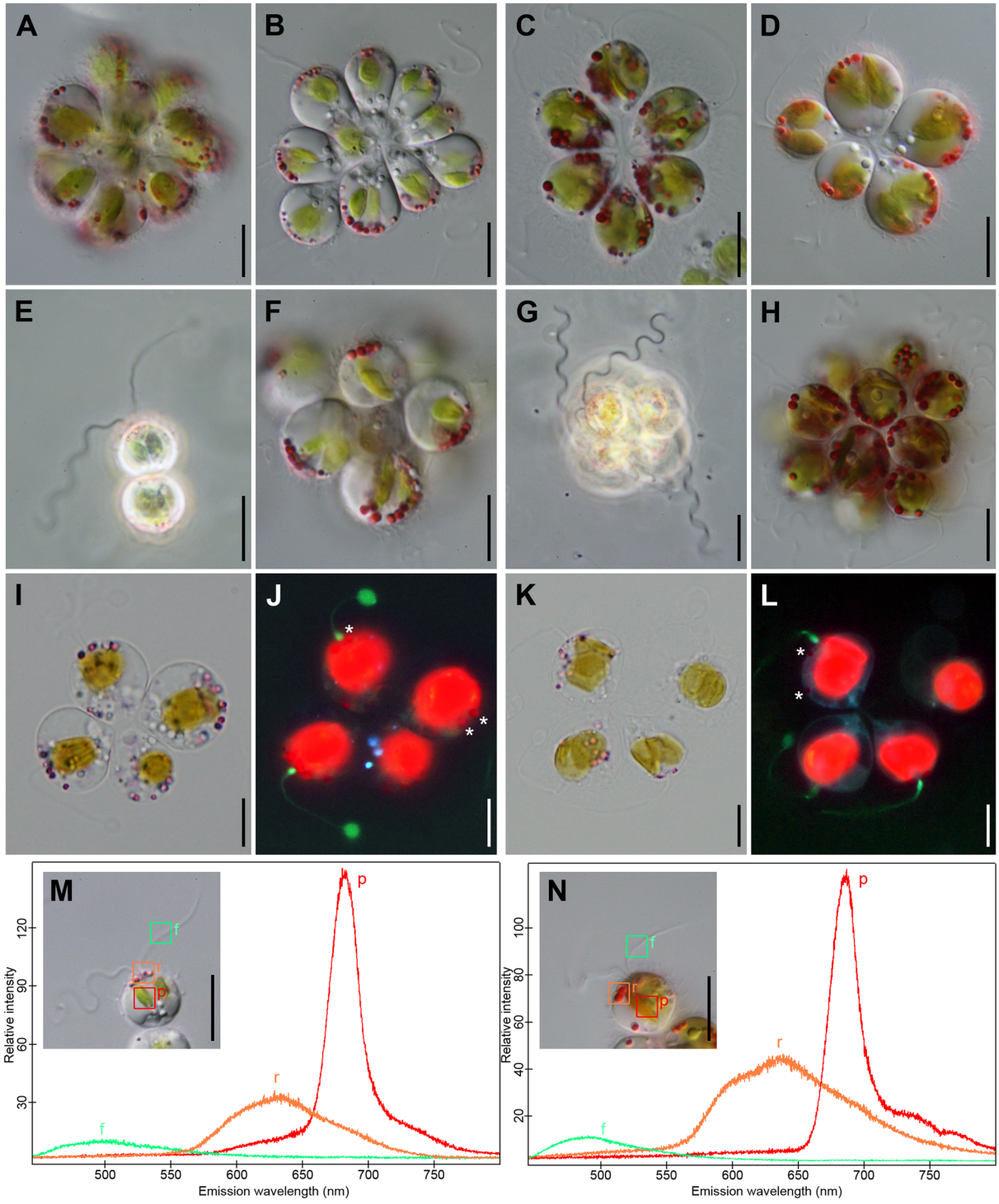

Fig. 5. Light microscopy and autofluorescence. (A–H) Morphology of colonies (A, B, E, F – sp1: *S. rubra*, sp. nov., C, D, G, H – sp2: *S. sphagnicola*); note typical Stramenopile flagella in E, G visualized by phase contrast; (I–L) light and autofluorescence pictures of four–celled colonies (I, J – sp1: *S. rubra*, sp. nov., K, L – sp2: *S. sphagnicola*); (M–N) autofluorescence emission spectra of plastids (in red), red droplets (in orange) and flagella (in green); investigated cells are shown in insets, showing the measured areas by squares of corresponding colours (M – sp1: *S. rubra*, sp. nov., N – sp2: *S. sphagnicola*). Scale bars represent 10 µm.

Pigment composition

The carotenoid composition found in *Synura sphagnicola* and *S. rubra* sp. nov. was typical of chrysophytes: fucoxanthin as the predominant carotenoid, and neoxanthin, zeaxanthin and b–carotene as minor carotenoids (Whiters et al. 1981). Surprisingly, chlorophyll $–c_1$ was not detectable both in *Synura sphagnicola* and *S. rubra* sp. nov., and chlorophyll–c_2 was identified in *S. sphagnicola.* According to Andersen & Mulkey (1983) chlorophyll–c_2 is missing in the genera *Synura* and *Mallomonas* Perty, where it is replaced by chlorophyll– c_1. Indeed, the lack of chlorophyll–c_2 was mentioned among major distinguishing

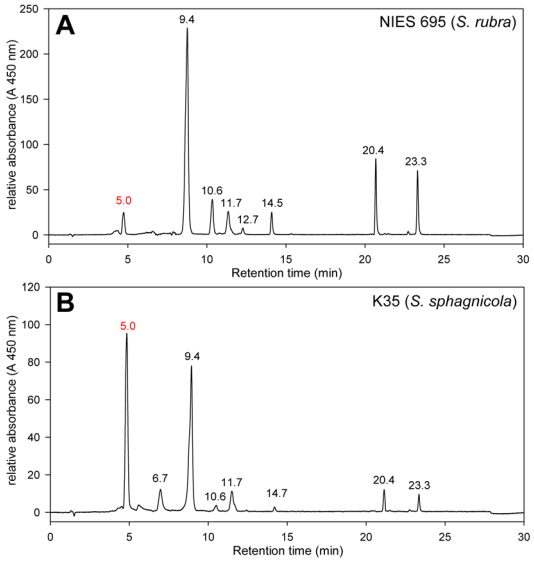

Fig. 6. Elution profiles of pigments extracted from cells of (A) sp1 (*S. rubra*, sp. nov.) and (B) sp2 (*S. sphagnicola*) lineages. Individual pigments are labelled by retention times (Rt). An unknown pigment with Rt = 5.0 is given in red colour.

characters to discriminate between classes Synurophyceae and Chrysophyceae (ANDERSEN 1987; 2010). However, FAWLEY (1989) found a new chlorophyll–c_2–like pigment in one culture of *S. petersenii.* Later on, with the development of more sensitive HPLC methods a new chlorophyll–c diversity was found in several groups of algae, including three chrysophyte species (ZAPATA et al. 2006). Interestingly, these authors already reported the presence of chlorophyll–c_2 in *S. sphagnicola*, in addition to a novel chlorophyll–c_2–like pigment of *Pavlova gyrans* type (ZAPATA et al. 2006). Finally, BOENIGK et al. (2023) recently reported the presence of chlorophyll– c_2 in five *Mallomonas* and four *Synura* taxa investigated. Accordingly, the pigment composition can no longer be used to define Synurophyceae. In addition, several recently published phylogenies show Synurophyceae to be nested within Chrysophyceae and referred to as the order Synurales Andersen (e.g., DEL CAMPO & MASSANA 2011; YANG et al. 2012; ŠKALOUD et al. 2013; SCOBLE & CAVALIER–SMITH 2014; KRISTIANSEN & ŠKALOUD 2017). Since there is no justification to recognize Synurales as a separate class Synurophyceae, we formally synonymize it with Chrysophyceae (see Taxonomic revisions and diagnoses below).

One of the most interesting results of pigment composition analysis is the discovery of the unknown pigment with Rt = 5.0 min. Since this pigment was dominant in the strain K35 characterized by a significant production of red droplets, we propose that the red droplets are formed from this newly recognized pigment. Various algae are known to produce red–coloured pigments (GRUNG & LIAAEN–JENSEN 1993; FRASSANITO 2006; LEMOINE & SCHOEFS 2010; LIU et al. 2014) including the industrially relevant species *Haematococcus pluvialis* used for aquaculture and cosmetics industries (BUBRICK 1991; LORENZ & CYSEWSKI 2000; TOMINAGA et al. 2012). In all above mentioned cases this pigment is astaxanthin, a pigment that belongs to the family of the xanthophylls, the oxygenated derivatives of carotenoids. However, we did not detect astaxanthin in either of the investigated strains. Astaxanthin is reported to have a peak emission at ~675 nm (OTA et al. 2018), which is not in the range of the red droplets emission spectra we documented (630–640 nm; Fig. 5). Further characterization of this compound using other methods is still underway.

TAXONOMIC REVISIONS AND DIAGNOSES

Chrysophyceae Pascher
Synonym: Synurophyceae ANDERSEN 1987; Am. J. Bot. 74(3): 338.
Description: Unicellular or colonial organisms with cells naked or surrounded by an envelope (cell wall, lorica, silica scales). Swarmers with two unequal flagella and contractile vacuoles. Longer flagellum hairy, shorter smooth. Cells can contain chloroplast derived from a red alga, with chlorophylls a, c_1 and/or c_2, but lacking chlorophyll–b. Fucoxanthin is the most important accessory pigment. Storage product β–1,3–glucan (chrysolaminaran). Known to form endogenous silicified cysts (statospores, stomatocysts) which are common in many geological deposits.

***Synura rubra* Škaloud, Škaloudová et Jadrná sp. nov.**
Description: Colonies are spherical, 29–34 µm in diameter, mostly composed of 8–16 cells. Cells are rounded, posteriorly tapering into the tail, 6–15(–17) µm in diameter. They possess pale green chloroplasts filling less than a half of the cell content, translucent droplets, and distinct red or red–violet droplets produced beneath the cell membrane. Each cell is surrounded by a distinct layer of spiny siliceous scales. Body scales are 2.5–5.3 µm long (mean 3.4 µm) and 1.7–3.3 µm wide (mean 2.4 µm), consisting of a basal plate with a spine. The basal plate is perforated by numerous pores and possess a posterior thickened rim encircling half to two–thirds of the scale perimeter, 0.1–0.4 µm in width. Spine is 0.8–2.6 µm long (mean 1.6 µm) and 0.1–0.5 µm wide (mean 0.3 µm), with distal end rounded or bearing two small teeth on the tip. Tubular scales are linear or slightly bent, up to 6.2 µm in length.

Etymology: The name refers to the reddish colour of the cells caused by the production of red pigment.
Holotype (here designated): Portion of a single gathering of cells on TEM grid NIES 695, deposited at the Culture Collection of Algae of Charles University in Prague, Czech Republic (CAUP). Fig. 7A is a representative scale from the specimen.
Strain information: The live culture of the holotype is deposited as NIES 695 at the Microbial Culture

Collection at the National Institute for Environmental Studies, Tsukuba, Japan.
Type locality: Miyatoko Mire, Fukushima, Japan (37°15'2.1" N, 139°33'56.3" E).

***Synura rubra* subsp. *rubra* (genotype sp1E, Figs 7A, B)**
Description: Colonies are spherical, composed of rounded cells posteriorly tapering into the tail. Cells surrounded by a distinct layer of spiny siliceous scales. Body scales are 2.0–2.8 µm long and 1.5–2.5 µm wide, consisting of a basal plate with a spine. A basal perforated plate strengthened by a posterior rim, 0.1–0.4 µm in width. Spine is 0.5–1.9 µm long and 0.2–0.4 µm wide.

Distribution: So far known only from Japan.
Ecology: Prefers humid climate (annual precipitation ~ 1.700 mm.year^{-1}) and more acidic habitats (pH ~ 5.0).

***Synura rubra* subsp. *ampla* Škaloud, Škaloudová et Jadrná subsp. nov. (genotype sp1AB, Figs 7C, D)**
Description: Colonies are spherical, composed of rounded cells posteriorly tapering into the tail. Cells surrounded by a distinct layer of spiny siliceous scales. Body scales are 2.5–5.3 µm long and 1.9–3.3 µm wide, consisting of a basal plate with a spine. A basal perforated plate strengthened by a posterior rim, 0.1–0.3 µm in width. Spine is 0.8–2.4 µm long and 0.1–0.5 µm wide.

Etymology: The name "ampla" (Latin), meaning wide or common, is used as an adjective in reference to the common occurrence of this subspecies.
Holotype (here designated): Portion of a single gathering of cells on TEM grid S71.G5, deposited at the Culture Collection of Algae of Charles University in Prague, Czech Republic (CAUP). Fig. 7C is a representative scale from the specimen.
Type locality: Borkovická blata, Czech Republic (49°14'8" N, 14°37'25.2" E).
Distribution: Restricted to Europe (Czech Republic, Sweden, United Kingdom, Ireland).
Ecology: Prefers drier climate (annual precipitation ~ 700–900(–1300) mm.year^{-1}) and more acidic habitats (pH ~ 5.0–5.2).

***Synura rubra* subsp. *bella* Škaloud, Škaloudová et Jadrná subsp. nov. (genotype sp1C, Figs 7E, F)**
Description: Colonies are spherical, composed of rounded cells posteriorly tapering into the tail. Cells surrounded by a distinct layer of spiny siliceous scales. Body scales are 2.0–3.0 µm long and 1.3–2.0 µm wide, consisting of a basal plate with a spine. A basal perforated plate strengthened by a posterior rim, 0.1–0.3 µm in width. Spine is 0.9–2.3 µm long and 0.2–0.3 µm wide.

Etymology: The name "bella" (Latin), meaning pretty or lovely, is used as an adjective in reference to the beautiful coloration of this subspecies.
Holotype (here designated): Portion of a single gathering of cells on TEM grid Juam032509D, deposited at the Culture Collection of Algae of Charles University in Prague, Czech Republic (CAUP Fig. 7E is a representative scale from the specimen.
Type locality: Dam Juam, Juam–myeon, Korea (34°59'21.5" N, 127°13'43.1" E).
Distribution: So far known only from South Korea.
Ecology: Prefers less acidic habitats (pH ~ 5.6) and environments showing high differences between day and night temperatures (mean diurnal range ~ 11 °C).

***Synura rubra* subsp. *caelica* Škaloud, Škaloudová et Jadrná subsp. nov. (genotype sp1D, Figs 7G, H)**
Description: Colonies are spherical, composed of rounded cells posteriorly tapering into the tail. Cells surrounded by a distinct layer of spiny siliceous scales. Body scales are 2.2–3.0 µm long and 1.7–2.4 µm wide, consisting of a basal plate with a spine. A basal perforated plate strengthened by a posterior rim, 0.1–0.3 µm in width. Spine is 0.7–2.3 µm long and 0.2–0.4 µm wide.

Etymology: The name "caelica" (Latin), meaning heavenly or magnificent, is used as an adjective in reference to the splendid appearance of this subspecies.
Holotype (here designated): Portion of a single gathering of cells on TEM grid CNU52, deposited at the Culture Collection of Algae of Charles University in Prague, Czech Republic (CAUP). Fig. 7G is a representative scale from the specimen.
Type locality: Beseokje, Gochang–gun, Korea (35°21'20.7" N, 126°33'27.4" E).
Distribution: So far known only from South Korea.
Ecology: Prefers less acidic habitats (pH ~ 5.6) and environments showing smaller differences between day and night temperatures (mean diurnal range ~ 7–9 °C).

***Synura sphagnicola* (Korshikov) Korshikov**
Synonym: *Synura bioretii* Huber–Pestalozzi 1941; Das Phytoplankton des Susswassers. 2,1: 141, Fig. 197 (as '*bioreti*').
Description: Colonies are spherical, 32–40 µm in diameter, mostly composed of 8–16 cells. Cells are rounded, posteriorly tapering into the tail, 10–17(–18) µm in diameter. They possess pale green to brownish chloroplasts filling at least half of the cell content, translucent droplets, and distinct red or red–violet droplets produced beneath the cell membrane. Each cell is surrounded by a distinct layer of spiny siliceous scales. Body scales are 2.4–4.8 µm long (mean 3.8 µm) and 1.9–4.0 µm wide (mean 2.8 µm), consisting of a basal plate with a spine. The basal plate is perforated by numerous pores and possess a posterior thickened rim encircling half to two–thirds of the scale perimeter, 0.1–0.6 µm in width. Spine is 0.8–4.1 µm long (mean 2.6 µm) and 0.1–0.6 µm wide (mean 0.3 µm), with a blunt distal end bearing 2–3, rarely 4 small teeth. Tubular scales present.

Type locality: Peat bogs near Zvenigorod, Russia (~ 55°41'56" N, 36°43'23" E).

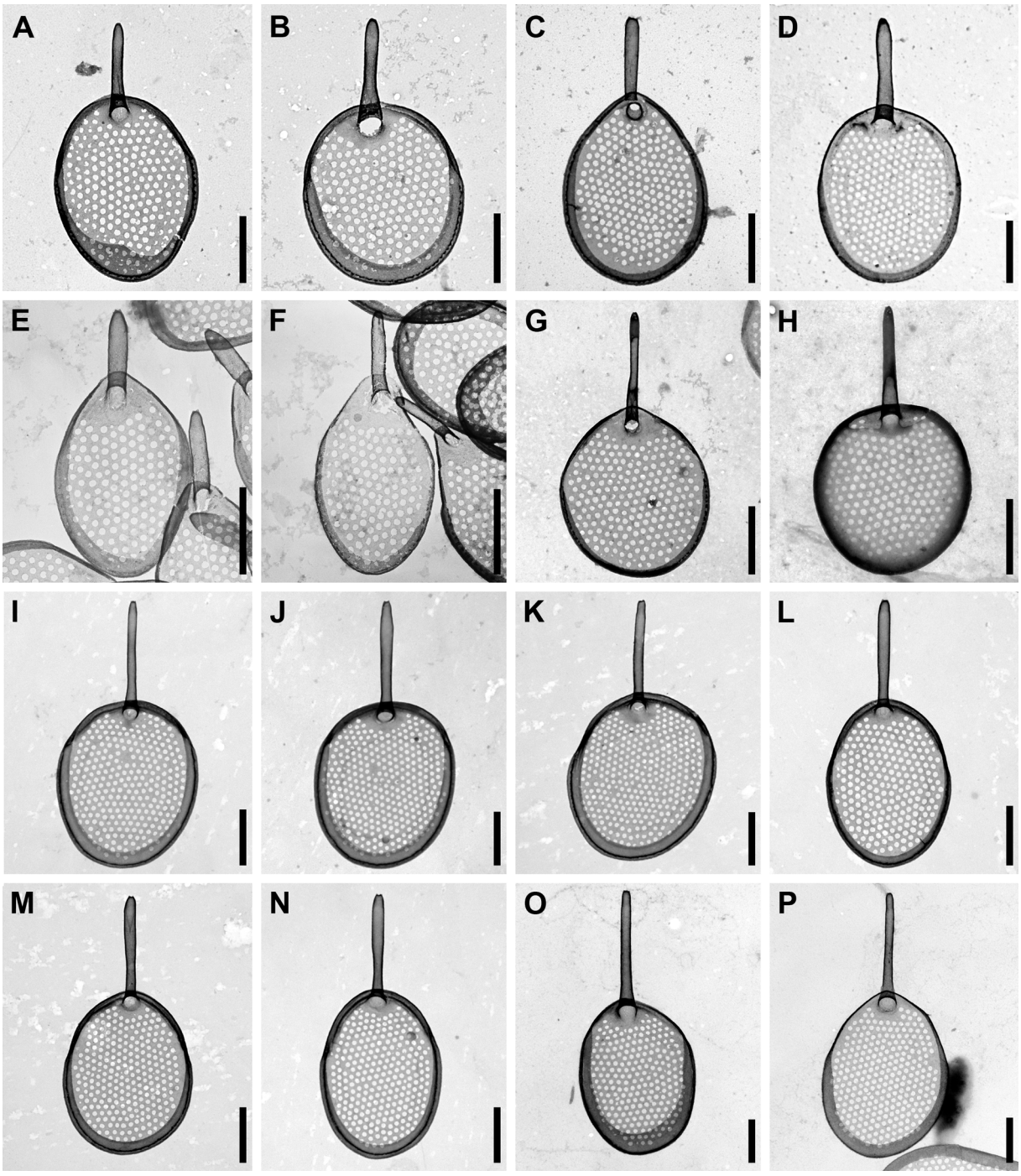

Fig. 7. Morphology of silica scales. (A–H) sp1: *S. rubra*, sp. nov.; (I–P) sp2: *S. sphagnicola*. (A–B) *S. rubra* subsp. *rubra* (strain NIES 695); (C–D) *Synura rubra* subsp. *ampla* (strains S71.G5 and S117.E4); (E–F) *Synura rubra* subsp. *bella* (strain Juam032509D); (G–H) *Synura rubra* subsp. *caelica* (strain CNU52); (I–K) *Synura sphagnicola* subsp. *sphagnicola* (strain M44); (L–N) *Synura sphagnicola* subsp. *agilis* (strain K35); (O–P) *Synura sphagnicola* subsp. *borealis* (strain S95.F9). Scale bars represent 1 µm.

***Synura sphagnicola* subsp. *sphagnicola* (genotype sp2B, Figs 7I–K)**

Description: Colonies are spherical, composed of rounded cells posteriorly tapering into the tail. Cells surrounded by a distinct layer of spiny siliceous scales. Body scales are 2.8–3.4 µm long and 2.1–2.8 µm wide, consisting of a basal plate with a spine. A basal perforated plate strengthened by a posterior rim, 0.2–0.4 µm in width. Spine is 1.5–2.4 µm long and 0.2–0.3 µm wide.

Distribution: Czech Republic, Norway, Canada, Russia.

Ecology: Prefers environments showing high differences between the hottest and the coldest months (temperature annual range ~ 28–35 °C) and habitats with low organic carbon stock (~ 50–58 g.kg^{-1}).

***Synura sphagnicola* subsp. *agilis* Škaloud, Škaloudová et Jadrná subsp. nov. (genotype sp2A, Figs 7L–N)**

Description: Colonies are spherical, composed of rounded cells posteriorly tapering into the tail. Cells surrounded by a distinct layer of spiny siliceous scales. Body scales are 2.6–4.8 µm long and 1.9–4.0 µm wide, consisting of a basal plate with a spine. A basal perforated plate strengthened by a posterior rim, 0.1–0.6 µm in width. Spine is 1.3–2.9 µm long and 0.2–0.5 µm wide.

Etymology: The name "agilis" (Latin), meaning agile or moving, is used as an adjective in reference to its swimming motion.

Holotype (here designated): Portion of a single gathering of cells on TEM grid K35, deposited at the Culture Collection of Algae of Charles University in Prague, Czech Republic (CAUP). Fig. 7L is a representative scale from the specimen.

Type locality: Jizerské hory, Czech Republic (50°50'14.2" N, 15°14'45.8" E).

Distribution: Czech Republic, United Kingdom.

Ecology: Occurred in moderately humid climate (annual precipitation ~ 800–1,200 mm, precipitation of wettest month ~ 100–150 mm.year^{-1}) and habitats with high organic carbon stock (~ 65 g.kg^{-1}).

***Synura sphagnicola* subsp. *borealis* Škaloud, Škaloudová et Jadrná subsp. nov. (genotype sp2C, Figs 7O, P)**

Description: Colonies are spherical, composed of rounded cells posteriorly tapering into the tail. Cells surrounded by a distinct layer of spiny siliceous scales. Body scales are 3.4–4.8 µm long and 2.1–3.8 µm wide, consisting of a basal plate with a spine. A basal perforated plate strengthened by a posterior rim, 0.2–0.6 µm in width. Spine is 1.7–4.1 µm long and 0.2–0.6 µm wide.

Etymology: The name "borealis" (Latin), meaning northern, is used as an adjective in reference to the presence of this subspecies in Northern Europe.

Holotype (here designated): Portion of a single gathering of cells on TEM grid S95.F9, deposited at the Culture Collection of Algae of Charles University in Prague, Czech Republic (CAUP). Fig. 7O is a representative scale from the specimen.

Type locality: Loch Carrie, Scotland, United Kingdom (57°21'32.6" N, 4°52'46.3" W).

Distribution: Sweden, Norway, United Kingdom.

Ecology: Prefers more humid climate (annual precipitation ~ 1,200–1,500 mm, precipitation of wettest month ~ 150–180 mm.year^{-1}) and habitats with high organic carbon stock (~ 60–80 g.kg^{-1}).

Acknowledgements

The study was supported by the Czech Science Foundation (project No. 20–22346S) and European Regional Development Fund and the state budget of the Czech Republic (project No. CZ.1.05/4.1.00/16.0340).

References

Andersen, R.A. (1987): Synurophyceae classis nov., a new class of algae. – American Journal of Botany 74: 337–353.

Andersen, R.A. (2010): Chapter 11. Chrysophyta. – In: Algae: Source to Treatment. AWWA Manual M57. – pp. 249–270, American Water Works Association, Denver.

Andersen, R.A.; Berges, J.; Harirson, P. & Watanabe, M. (2005): Appendix A – recipes for freshwater and seawater media. – In: Andersen, R.A. (ed.): Algal Culturing Techniques, – pp. 429–538, Elsevier, Amsterdam, the Netherlands.

Andersen, R.A. & Mulkey, T.J. (1983): The occurrence of chlorophylls c_1 and c_2 in the Chrysophyceae. – Journal of Phycology 19: 289–294.

Annenkova, N.V.; Hansen, G.; Moestrup, Ø. & Rengefors, K. (2015): Recent radiation in a marine and freshwater dinoflagellate species flock. – ISME Journal 9: 1821–1834.

Boenigk, J., Beisser, D., Franke, L., Klar, L., Ilić, M. & Fink, P. (2023): Differences in pigment composition and concentration between phototrophic, mixotrophic and heterotrophic Chrysophyceae. – Fottea (this issue). DOI: 10.5507/fot.2023.001

Bouckaert, R.R. (2010): DensiTree making sense of sets of phylogenetic trees. – Bioinformatics 26 (10): 1372–1373.

Bouckaert, R.; Heled, J.; Kühnert, D; Vaughan, T.; Wu, C.H.; Xie, D.; Suchard, M.A.; Rambaut, A. & Drummond, A.J. (2014): BEAST 2: A Software Platform for Bayesian Evolutionary Analysis. – PLOS Computational Biology 10(4): e1003537.

Bubrick, P. (1991): Production of astaxanthin from *Haematococcus*. – Bioresource Technology 38: 237–239.

del Campo, J. & Massana, R. (2011): Emerging diversity within chrysophytes, choanoflagellates and bicosoecids based on molecular surveys. – Protist 162(3): 435–48.

Conrad, W. (1939): Notes Protistologiques. VIII. *Synura sphagnicola* Korsch. en Belgique. – Bull. Inst. r. Sci. nat. Belq. 15(4): 1–4.

Donaldson, L. (2020): Autofluorescence in plants. – Molecules 25(10): 1–20.

Fawley, M.W. (1989): A new form of chlorophyll c involved in light–harvesting. – Plant Physiology 91: 727–732.

Frassanito, R.; Flaim, G.; Mancini, I. & Guella, G. (2006): High production of unexpected carotenoids in Dinophyceae. Astaxanthin esters from the freshwater dinoflagellate *Tovellia sanguinea*. – Biochemical Systematics and Ecology 34: 843–853.

Fricano, A.; Librizzi, F.; Rao, E.; Alfano, C. & Vetri, V. (2019): Blue autofluorescence in protein aggregates "lighted on" by UV induced oxidation. – Biochimica et Biophysica Acta (BBA) – Proteins and Proteomics 1867(11): 1–10.

Fujita, S.; Iseki, M.; Yoshikawa, S.; Makino, Y.; Watanabe, M.; Motomura, T.; Kawai, H. & Murakami, A. (2005): Identificationand characterization of a fluorescent flagellar protein from the brown alga *Scytosiphon lomentaria* (Scytosiphonales, Phaeophyceae): A flavoprotein homologous to Old Yellow Enzyme. – European Journal of Phycology 40: 159–167.

Graham, L.E.; Graham, J.M. & Wujek, D.E. (1993): Ultrastructure of *Chrysodidymus synuroideus* (Synurophyceae). – Journal of Phycology 29: 330–341.

Grung, M. & Liaaen–Jensen, S. (1993): Algal carotenoids 52*; secondary carotenoids of algae 3; carotenoids in a natural bloom of *Euglena sanguinea*. – Biochemical

Systematics and Ecology 21(8):757–763.

Harris, K. & Bradley, D.E. (1958): Some unusual Chrysophyceae studied in the electron microscope. – Journal of General Microbiology 18: 71–83.

Hewitt, G. (2000): The genetic legacy of the quaternary ice ages. – Nature 405: 907–913.

Hibberd, D.J. (1978): The fine structure of *Synura sphagnicola* (Korsh.) Korsh. (Chrysophyceae). – British Phycological Journal 13: 403–412.

Hijmans, R.J.; Cameron, S.E.; Parra, J.L.; Jones, P.G. & Jarvis, A. (2005): Very high resolution interpolated climate surfaces for global land areas. – International Journal of Climatology 25: 1965–1978.

Huang, S.; Heikal, A.A. & Webb, W.W. (2002): Two–photon fluorescence spectroscopy and microscopy of NAD(P)H and flavoprotein. – Biophysical Journal 82: 2811–2825.

Huber–Pestalozzi, G. (1941): Das Phytoplankton des Susswassers. 2,1. Chrysophyceen, farblose Flagellaten, Heterokonten. – In: Thienemann, A. (ed.): Die Binnengewasser XVI, 2, 1. – 365 pp., Schweizerbartsche Verlagsbuchbehandlung, Stuttgart.

Jo, B.Y.; Kim, J.I.; Skaloud, P.; Siver, P.A. & Shin, W. (2016): Multigene phylogeny of *Synura* (Synurophyceae) and descriptions of four new species based on morphological and DNA evidence. – European Journal of Phycology 51: 413–30.

Katoh, K.; Misawa, K.; Kuma, K. & Miyata, T. (2002): MAFFT: a novel method for rapid multiple sequence alignment based on fast Fourier transform. – Nucleic Acid Research 30: 3059–3066.

Kawai, H. (1988): A flavin–like autofluorescent substance in the posterior flagellum of golden and brown algae. – Journal of Phycology 24: 114–117.

Korshikov, A.A. (1927): *Skadovskiella sphagnicola*, a new colonial Chrysomonad. – Archiv für Protistenkunde 58: 450–455.

Korshikov, A.A. (1929): Studies on the Chrysomonads. I. – Archiv für Protistenkunde 67: 253–290.

Kreimer, G. (1994): Cell biology of phototaxis in flagellate algae. – International Review of Cytology: 229–310.

Kristiansen, J. & Preisig, H.R. (2007): Chrysophyte and Haptophyte Algae, 2nd part. Synurophyceae. In: Büdel, B., Gärtner, G., Krienitz, L., Preisig, H.R. & Schagerl, M. (eds.) Süsswasserflora von Mitteleuropa 1/2. Springer–Verlag, Berlin, 252 pp.

Kristiansen, J. & Skaloud, P. (2017): Chrysophyta. – In: Archibald, J. M.; Simpson, A.G.B. & Slamovits, C.H. (eds): Handbook of the Protists: Second Edition. – pp. 331–366, Springer International Publishing, Cham, Switzerland.

Lemoine, Y. & Schoefs, B. (2010): Secondary ketocarotenoid astaxanthin biosynthesis in algae: a multifunctional response to stress. – Photosynthesis Research 106: 155–177.

Liu, J., Z. Sun, H. Gerken, Z. Liu, Y. Jiang, and F. Chen (2014): *Chlorella zofingiensis* as an alternative microalgal producer of astaxanthin: Biology and industrial potential. – Marine Drugs 12: 3487–3515.

Logares, R.; Rengefors, K.; Kremp, A.; Shalchian–Tabrizi, K.; Boltovskoy, A.; Tengs, T.; Shurtleff, A. & Klaveness, D. (2007): Phenotypically different microalgal morphospecies with identical ribosomal DNA: a case of rapid adaptive evolution? – Microbial Ecology 53(4): 549–561.

Lorenz, R.T. & Cysewski, G.R. (2000): Commercial potential for *Haematococcus* microalgae as a natural source of astaxanthin. – Trends in Biotechnology 18:160–167.

Oksanen, J.; Blanchet, F.G.; Friendly, M.; Kindt, R.; Legendre, P.; McGlinn, D.; Minchin, P.R.;. O'Hara, R.B.; Simpson, G.L.; Solymos, P.; Stevens, M.H.H.; Szoecs, E. & Wagner, H. (2020): vegan: Community Ecology Package. R package version 2.5–7, from https://CRAN.R–project.org/package=vegan.

Ota, S.; Morita, A.; Ohnuki, S.; Hirata, A.; Sekida, S.; Okuda, K.; Ohya, Y. & Kawano, S.J. (2018): Carotenoid dynamics and lipid droplet containing astaxanthin in response to light in the green alga *Haematococcus pluvialis*. – Scientific Reports 8: 5617.

Petersen, J.B. & Hansen, J.B. (1958). On the scales of some *Synura* species, II. – Biologiske Meddelelser, Kongelige Danske. Videnskabernes Selskab 23(7): 1–13.

Pusztai, M.; Certnerova, D.; Skaloudova, M. & Skaloud, P. (2016): Elucidating the phylogeny and taxonomic position of the genus *Chrysodidymus* Prowse (Chrysophyceae, Synurales). – Cryptogamie Algologie 37: 297–307.

R Core Team (2021): R: A language and environment for statistical computing. R Foundation for Statistical Computing, Vienna, Austria. Available at: https://www.R–project.org/.

Roberts, D.W. (2019): labdsv: Ordination and Multivariate Analysis for Ecology. R package version 2.0–1. from https://CRAN.R–project.org/package=labdsv.

Roshchina, V.V. (2012): Vital autofluorescence: application to the study of plant living cells. –International Journal of Spectroscopy: 1–14.

Ronquist, F.; Teslenko, M.; van der Mark, P.; Ayres, D.L.; Darling, A.; Höhna, S.; Larget, B.; Liu, L.; Suchard, M.A. & Huelsenbeck, J.P. (2012): MrBayes 3.2: efficient Bayesian phylogenetic inference and model choice across a large model space. – Systematic Biology 61(3): 539–542.

Scoble, J. M. & Cavalier–Smith, T. (2014): Scale evolution in paraphysomonadida (Chrysophyceae): Sequence phylogeny and revised taxonomy of *Paraphysomonas*, new genus *Clathromonas*, and 25 new species. – European Journal of Protistology 50(5): 551–592.

Silkina, A.; Bazes, A.; Vouvé, F.; Le Tilly, V.; Douzenel, P.; Mouget, J. L. & Bourgougnon, N. (2009): Antifouling activity of macroalgal extracts on *Fragilaria pinnata* (Bacillariophyceae): A comparison with Diuron. – Aquatic Toxicology 94(4): 245–254.

Siver, P.A. (1989): The distribution of scaled chrysophytes along a pH gradient. – Canadian Journal of Botany 67: 2120–2130.

Swofford, D.L. (2003): PAUP. Phylogenetic analysis using parsimony (and other methods). Version 4. Sinauer Associates, Sunderland.

Škaloud, P.; Kristiansen, J. & Škaloudová, M. (2013): Developments in the taxonomy of silica–scaled chrysophytes – from morphological and ultrastructural to molecular approaches. – Nordic Journal of Botany 31: 385–402.

Škaloud, P.; Škaloudová, M.; Doskočilová, P.; Kim, J.I.; Shin, W. & Dvořák, P. (2019): Speciation in protists: Spatial and ecological divergence processes cause rapid species diversification in a freshwater chrysophyte. – Molecular Ecology 28: 1084–1095.

Škaloud, P.; Škaloudová, M.; Jadrná, I.; Bestová, H.; Pusztai, M.; Kapustin, D. & Siver, P.A. (2020): Comparing morphological and molecular estimates

of species diversity in the freshwater genus *Synura* (Stramenopiles): A model for understanding diversity of eukaryotic microorganisms. – Journal of Phycology 56: 574–591.

Tominaga, K.; Hongo, N.; Karato, M. & Yamashita, E. (2012): Cosmetic benefits of astaxanthin on humans subjects. – Acta Biochimica Polonica 59: 43–47.

Van Heukelem, L. & Thomas, C.S. (2001): Computer–assisted high–performance liquid chromatography method development with applications to the isolation and analysis of phytoplankton pigments. – Journal of Chromatography A, 910(1): 31–49.

Venables, W.N. & Ripley, B.D. (2002): Modern Applied Statistics with S. Fourth Edition. Springer, New York.

Wickham, H. (2016): ggplot2: Elegant Graphics for Data Analysis. Springer–Verlag New York.

Wilke, C.O. (2021): ggridges: Ridgeline Plots in ‚ggplot2'. R package version 0.5.3. from https://CRAN.R–project.org/package=ggridges.

Withers, N.W.; Fiksdahl, A.; Tuttle, R.C. & Liaaen–Jensen, S. (1981): Carotenoids of the Chrysophyceae. – Comparative Biochemistry and Physiology 68B: 345–349.

Yang, E.C.; Boo, G.H.; Kim, H.J.; Cho, S.M.; Boo, S. M.; Andersen, R.A. & Yoon, H.S. (2012): Supermatrix data highlight the phylogenetic relationships of photosynthetic Stramenopiles. – Protist 163: 217–231.

Zapata, M.; Garrido, J.L. & Jeffrey, S.W. (2006): Chapter 3. Chlorophyll c Pigments: Current Status. – In: Grimm, B.; Porra, R.J.; Rüdiger, W. & Scheer, H. (eds): Chlorophylls and Bacteriochlorophylls. Advances in Photosynthesis and Respiration, vol 25. – pp. 39–53, Springer, Dordrecht.

Supplementary material

The following supplementary material is available for this article:

Table S1. List of taxa, sampling details and GenBank accession numbers for sequences analysed for Figure 1A.

Table S2. List of taxa, sampling details and GenBank accession numbers for sequences analysed for Figure 1B.

This material is available as part of the online article (http://fottea.czechphycology.cz/contents)

Received July 26, 2022
Accepted December 15, 2022